Multifrequency Microstrip Antennas Using Alumina-Ceramic/Polyimide Multilayer Dielectric Substrate

Kenji Kamogawa, *Member, IEEE*, Tsuneo Tokumitsu, *Member, IEEE*, and Masayoshi Aikawa, *Member, IEEE*

***Abstract*— A novel microstrip antenna using an alumina-ceramic/polyimide multilayer dielectric substrate is presented. The multilayer configuration, in which two different multilayer materials with much different permittivities and thicknesses are stacked together, can be used for designing an antenna with selective substrate thickness, thus providing the optimum substrate thickness for the desired frequency. Both 10 GHz-band and 18 GHz-band antennas are designed and fabricated on the same substrate to demonstrate this feature. They achieve perfect matching and acceptable radiation characteristics. Furthermore, for application to array antennas, power combining circuits such as a 90° hybrid and a four-port divider are demonstrated. Finally, the possibility of applying this technology to active antenna systems is discussed. The measurement results confirm that the proposed multilayer substrate is extremely suitable for building active array systems integrated with active devices and monolithic microwave/millimeter wave integrated circuits (MMIC), as well as for constructing multifrequency antennas.**

I. Introduction

ACTIVE antennas integrated together with solid-state devices, feed circuits, and antennas on a single substrate, offer significant advantages in performance and cost for microwave and millimeter-wave wireless systems. Although several concepts of using microstrip antennas as active antennas have been reported [1]–[4], microstrip antennas are primarily single-frequency and narrow-band antennas. Dual-frequency and multifrequency operations are possible approaches to widen the bandwidth against the limitation of microstrip antennas [5]–[8]. However, frequency selectivity is still limited because of the fixed substrate thickness; i.e., the frequencies can not be arbitrarily selected. A multilayer substrate which allows a conductor plane to be placed on every layer, is an effective solution to overcome this problem. Therefore, a new microstrip antenna configuration using an alumina-ceramic/polyimide multilayer dielectric substrate has been proposed [9], [10]. The multilayer configuration in which two different multilayer materials with much different permittivities and thicknesses are stacked together, can be used for designing an antenna with selective substrate thickness, thus providing the optimum substrate thickness for the operation frequency or frequencies desired. Ceramic/polyimide multilayer substrates have been developed as a multichip module (MCM) substrate for VLSI chips [11], [12], and a substrate with combined thin film capacitors has already been reported [13]. All these results confirm the suitability of the ceramic/polyimide multilayer substrate for realizing active antennas systems integrated with active devices and monolithic microwave/millimeter wave integrated circuits (MMIC).

Manuscript received March 29, 1996.

The authors are with the NTT Wireless Systems Laboratories, 1-1 Hikarikooka, Yokosuka-shi, Kanagawa 239, Japan.

Publisher Item Identifier S 0018-9480(96)08567-5.

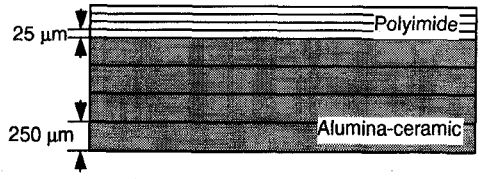

Fig. 1. Configuration of alumina-ceramic/polyimide multilayer dielectric substrate.

TABLE I
MULTILAYER DIELECTRIC PROPERTIES

	Alumina ceramic	Polymide
Permittivity (@ 10 GHz)	9.0	3.2
Loss Tangent (@ 10 GHz)	0.001	0.002
Thermal Expansion $\times 10^{-6}$/°C	6.8	20-70
Metallization material	W (tungsten)	Au (gold)

This paper first describes the features derived from the structure, and then microstrip antennas and power combining circuits such as a four-port divider and a 90° broadside coupler are demonstrated to confirm these features. Finally, we briefly discuss the possible benefits of integrating solid-state devices and/or MMIC's on the multilayer substrate for active antenna application. Both 10 GHz-band and 18 GHz-band patch antennas are fabricated and are found to achieve good performance. Passive circuits, manufactured using polyimide layers, have low-insertion-loss and wideband characteristics. According to measurement results and brief discussion of the active antenna application, the proposed multilayer configuration is shown to be extremely suitable as a multifrequncy antenna and for realizing active array systems in combination with active devices and MMIC's.

II. Structure and Features

Fig. 1 shows a multilayer dielectric substrate consisting of four alumina-ceramic and four polyimide layers [11], [13]. Each polyimide layer is 25 μm thick, and each alumina-ceramic layer is 250 μm thick. The characteristics of these materials are presented in Table I. The relative permittivity and loss tangent of the ceramic layers are 9.0 and 0.001 at 10 GHz, respectively, and those of the polyimide layers are 3.2 and 0.002, respectively. Although the two types of material have quite different thermal expansion coefficients (ceramic: 6.8×10^{-6}/°C, polyimide: 2070×10^{-6}/°C) the antennas and circuits manufactured on this substrate were found to be highly

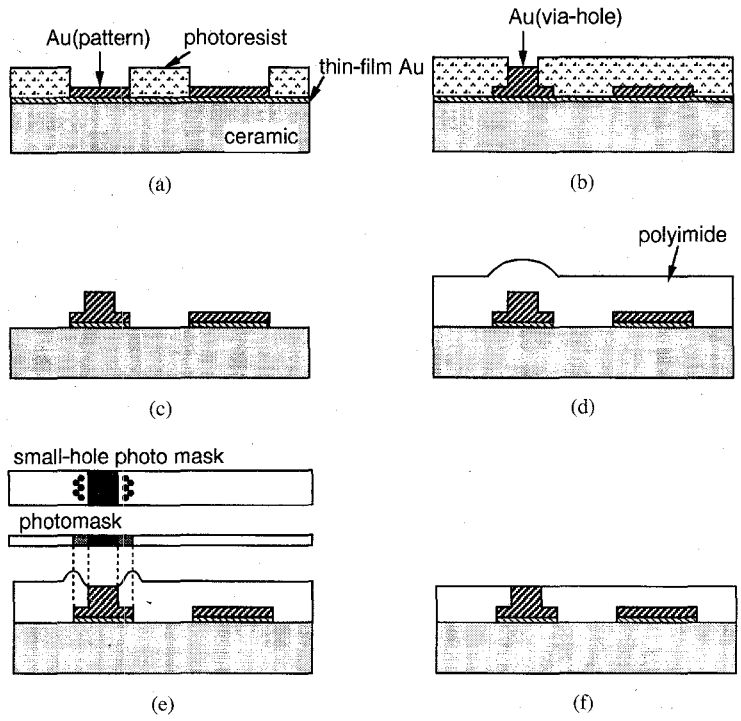

Fig. 2. Process flow of polyimide layers.

stable and reliable under 150°C, 85% r.h. (1.7 atm.), 1000-h pressure cooker test (PCT) and 1000 times, −65/150°C thermal cycle test (TCT). Gold and tungsten are used for the conductors on the polyimide and ceramic layers, respectively.

The antennas and circuits fabricated on the alumina-ceramic/polyimide multilayer substrate of Fig. 1, offer the following features.

1) Multifrequency antenna systems with optimum substrate thickness for each operation frequency can be designed because the multilayer substrate, consisting of two dielectric materials with much different permittivities and thicknesses, provide a wide range of effective thickness.
2) Each antenna performs well even at higher frequencies because the equivalent dielectric-constant is decreased by the reduced number of ceramic layers, as well as being small in the low frequency-bands.
3) The ceramic substrate is very suitable for integration with active devices and MMIC's because its thermal expansion coefficient (6.8×10^{-6}/°C) matches those of semiconductors such as GaAs (6.0×10^{-6}/°C) and Si (3.4×10^{-6}/°C).
4) The ceramics bending strength of 350 MPa is three and half times higher than that of Si substrates, and thus supports antenna arrays with a number of elements.
5) Owing to the characteristics of the multilayer substrate, the layout of the power combining circuits and bias circuits is more flexible, and the meander-like configuration and conductor crossovers can be used to reduce chip size.

III. Fabrication Process

Manufacturing the multilayer substrate shown in Fig. 1 proceeds in two main stages: the alumina-ceramic layer process and the Au-polyimide layer process. The ceramic process punches holes in a green tape for via holes, filling the holes with tungsten and printing the pattern desired. The green tape lamination is snapped and cut to the appropriate size, where the ceramic substrate is 10×10 cm^2 after firing at temperatures of more than 1450°C. After firing, the four-layer alumina-ceramic substrate is slightly cupped so its top and bottom surfaces are ground flat prior to Au-polyimide multilayer fabrication. The Au-polyimide structure, i.e., five-layer Au-metallization and four-layer polyimide, is manufactured by the photolithography technology [14]. The main steps of the one-layer fabrication process are shown in Fig. 2. A thin-film gold layer is formed by sputtering, followed by the photoresist coating and the patterning of the gold grown on the thin-film layer by electroplating, as shown in Fig. 2(a). After removing the resist, another resist is formed for patterning and brazing the via-holes [Fig. 2(b)]. The resist is again removed and the thin-film gold is etched as shown in Fig. 2(c). The polyimide layer is formed by double spin coating to form 12.5-μm polyimide [Fig. 2(d)]. Fig. 2(e) shows polyimide layer formation using specific photomasks. The final step is flattening and curing the polyimide for depositing the next layer, as shown in Fig. 2(f). The polyimide layers are not formed on the areas reserved for the on-wafer RF-probes and MMIC chips.

IV. Microstrip Antennas

The design of antennas utilizing features 1) and 2) are described in this section. The dielectric thickness of the microstrip antenna substrate is the most important design factor because it determines most of the antenna's characteristics such as gain, efficiency, and bandwidth [15], [16]. The substrate thickness versus operation frequency is shown in Fig. 3. The circles show the frequencies at which the multilayer

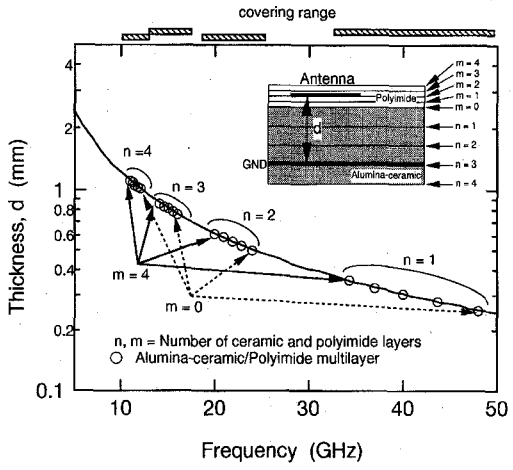

Fig. 3. Substrate thickness for suitable microstrip antenna design as a function of frequency. The circles show the frequencies at which four-layer alumina-ceramic and four-layer polyimide dielectric substrate can be used.

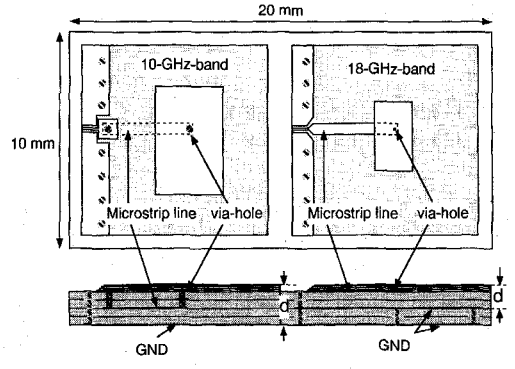

Fig. 4. Configuration of patch antennas using the multilayer substrate.

substrate shown in Fig. 1 can be used. The solid line (1/25 free space wavelength) indicates the substrate thicknesses typically used in conventional antenna designs. The alumina-ceramic/polyimide multilayer dielectric substrate can be used for designing antennas that offer optimum performance over a wideband frequency range, resulting in the possibility of using the fabrication process but with different masks to create multifrequency antennas on the same substrate. Frequency coverage can be improved by increasing the number of layers and making each layer thinner.

Fig. 4 shows the configuration of a 10 GHz-band and 18 GHz-band microstrip antenna. These antennas are directly fed by 50 μm radius via-holes connecting a 0.45 mm-wide microstrip line, which is joined to a coplanar waveguide (CPW) at the other terminal for on-wafer measurement. The feeding point is offset from the center of the patch to match the 50 Ω microstrip line. The 10 GHz-band and 18 GHz-band patches are, respectively, 5.0 mm and 3.2 mm long (resonant length), 3.0 mm and 1.8 mm wide. The offsets, calculated by SONNET Software, are 0.45 mm and 0.37 mm from the center as listed in Table II. The ground plane is formed at the bottom of the ceramic substrate for the 10 GHz-band antenna (effective substrate thickness: 1.1 mm), and at the middle of the substrate for the 18 GHz-band antenna (effective substrate thickness: 0.6 mm).

TABLE II
PARAMETERS OF PATCH ANTENNAS

	10 GHz-band	18 GHz-band
Length of patch, L	5 mm	3.2 mm
Width of patch, W	3 mm	1.8 mm
Thickness, d	1.1 mm	0.6 mm
Offset, s	0.45 mm	0.37 mm

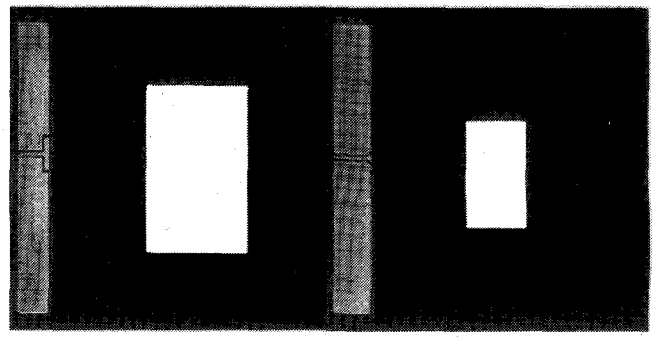

Fig. 5. Photograph of the fabricated 10 GHz-band and 20 GHz-band patches.

Fig. 5 shows a photograph of the fabricated 10 GHz-band and 18 GHz-band antennas. These fabricated antenna are located on one corner of the 10×10 cm^2 multilayer substrate, thus maximizing possible fabrication error. Fig. 6(a) and (b) show a Smith chart plot of the input impedance and return loss of the two antennas. Both of them achieve a perfect match at 10.43 GHz and 17.87 GHz, respectively; their return losses are less than -30 dB. The 18 GHz-band antenna has wider bandwidth than the 10 GHz-band antenna since it has a lower equivalent dielectric constant. Measured far-field patterns of the 10 GHz-band antenna are shown in Fig. 7. The antenna chip, 10×10 mm^2, was mounted on a 10×10 cm^2 copper plate for far-field measurement. The measured pattern is in good agreement with the pattern calculated by moment analysis assuming an infinite substrate [17]. The 4 dB ripple in the E-plane pattern is generated more by the edge effect of the two ground metals for CPW, than the copper ground plane.

V. POWER COMBINING CIRCUITS

Power combining circuits and feeder circuits, which employ feature 5), are discussed for antenna arrays and active antenna applications using the proposed multilayer substrate in this section. The most important design issue for these circuits is to provide low loss characteristics to eliminate excessive and expensive RF circuits, indicating low-cost and simple systems. Therefore, a fineline multilayer metallization consisting of four polyimide layers and five 5-μm-thick gold films, was used in the design of the feed circuits. Using thin film dielectric layers, the thin film microstrip (TFMS) line, shown in Fig. 8, is the most practical transmission line; one typical application of thin film dielectric layers is in three-dimensional (3-D) MMIC's [18]–[20]. The fundamental power combining circuits of a four-port divider and 90° broadside coupler, which consist of TFMS lines, were designed and simultaneously fabricated

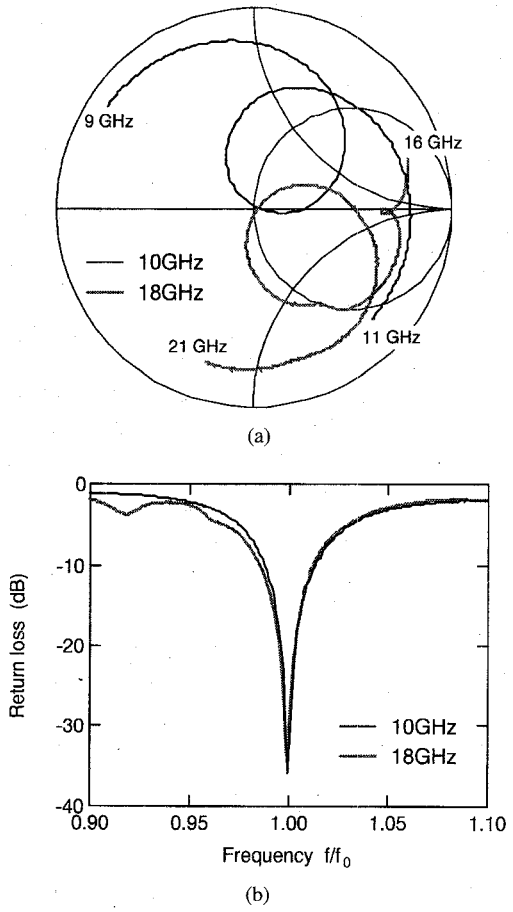

Fig. 6. Measured performance of patches: (a) Smith chart plots of the input impedance and (b) return loss.

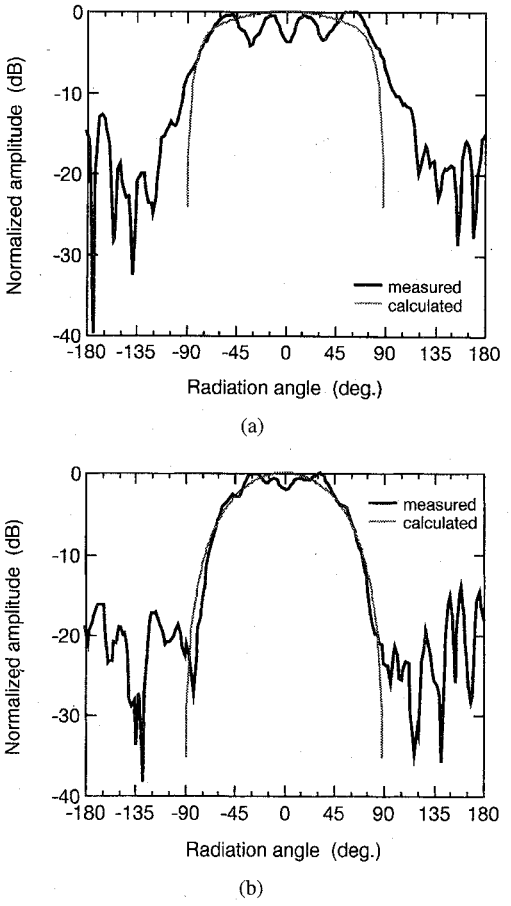

Fig. 7. Radiation pattern of the 10 GHz-band antenna: (a) E-plane and (b) H-plane.

with the antennas shown in Fig. 5 on the same substrate. The broadside coupler can also be used as a feeder for circular-polarization antennas.

A. Four-Port Divider

A four-port divider was designed by using the calculated characteristic impedance and normalized guided wavelength (λ_g/λ_0) of the TFMS lines as shown in Fig. 9(a). The parameters of the width and heights of conductor in Fig. 8 were used in this calculation. The characteristic impedance of TFMS lines varies between 10 and 130-Ω for conductor widths ranging from 25 to 250-μm, and are similar to the polyimide layer thickness. The guided wavelengths of lines in the polyimide layers are almost the same for the conductor width range of 25–250 μm. Fig. 9(b) shows the calculated loss characteristic as a function of conductor width at the frequency of 10 GHz. TFMS line losses moderately decrease as conductor width increases, and are less than from 1/10 to 1/2 those of lines on 3-D MMIC's [19]. Furthermore, the loss characteristic of TFMS lines on the lower polyimide layer is degraded by the dielectric loss.

Fig. 10 (a)–(c) show the circuit scheme, photograph and cross-sectional view of an 11 GHz four-port divider with chip size of 2.3 mm $\times$ 1.7 mm. The divider is based on an impedance transformer with neglible isolation between the output ports. A quarter-wavelength line of 25 Ω, 110 μm-width TFMS line and four 50 Ω, 50 μm-width TFMS lines are formed on the first 25 μm-thick polyimide layer and the second 50 μm-thick one, respectively. The quarter-wavelength of 3.8 mm is chosen by the calculation results plotted in Fig. 9(a). The measured and calculated input return loss and coupling characteristics are shown in Fig. 11. Good agreement between measured and calculated results is obtained. Coupling loss of 6 ± 0.5 dB, and return loss of less than -10 dB are obtained at frequencies between 6 GHz and 14 GHz. The power and phase dispersion of signals divided and passed to the output ports are within 0.4 dB and 4°, respectively, in the same frequency band. Furthermore, the four-port divider achieves a low insertion loss of 0.2 dB at 10 GHz.

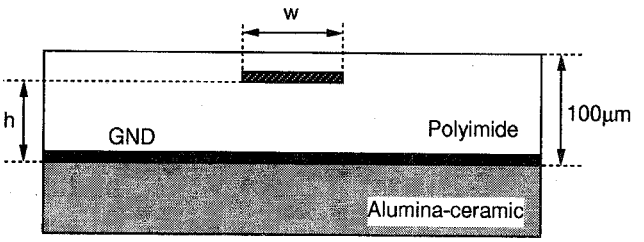

Fig. 8. Cross section of the TFMS line using polyimide layers.

B. 90-Degree Hybrid

Fig. 12(a) shows the cross-sectional view of a 90° hybrid (broadside coupler). In this figure, w_1, w_2, h_1, and h_2 are, re-

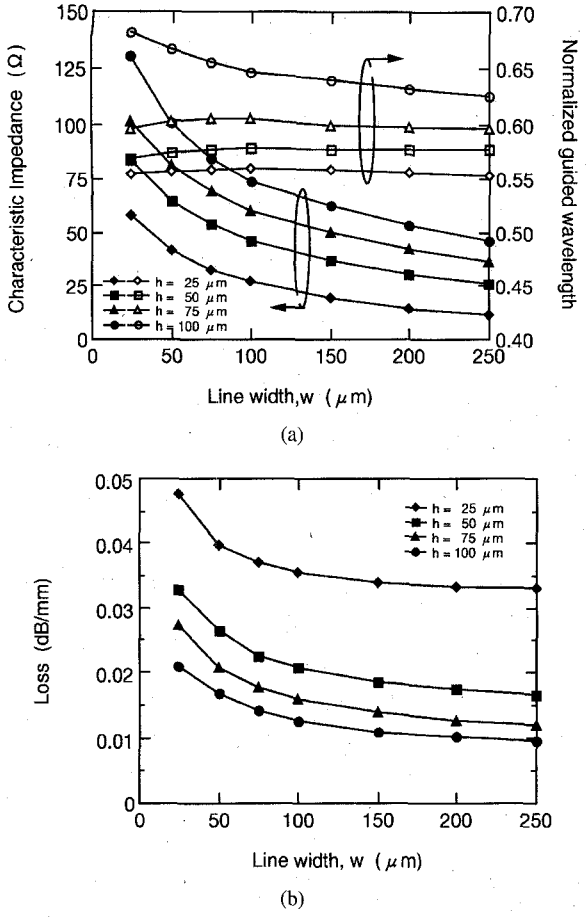

Fig. 9. Calculated characteristic impedance, normalized guided wavelength and loss of the TFMS lines.

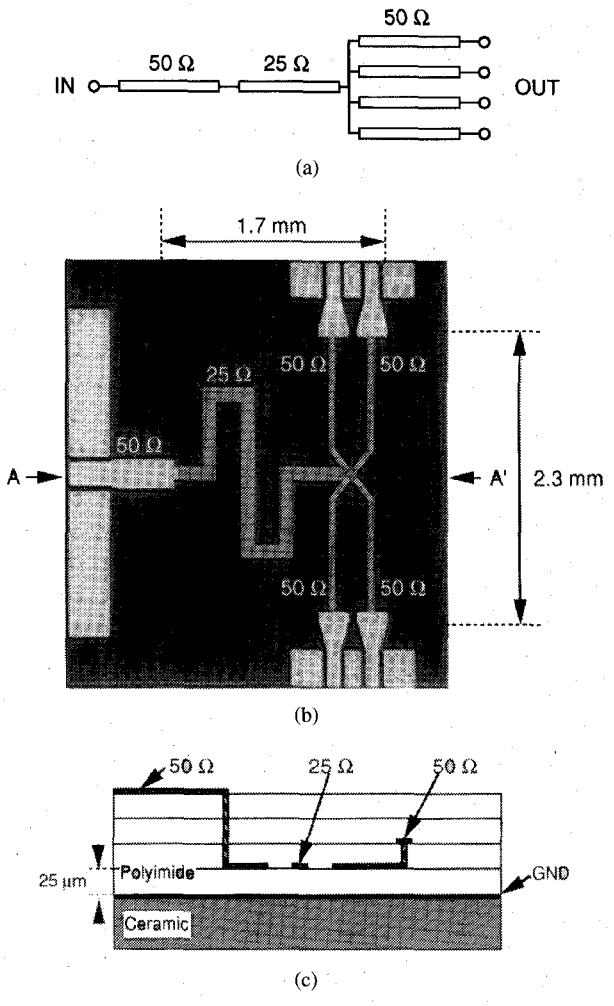

Fig. 10. Circuit scheme and photograph of the 11 GHz four-port divider.

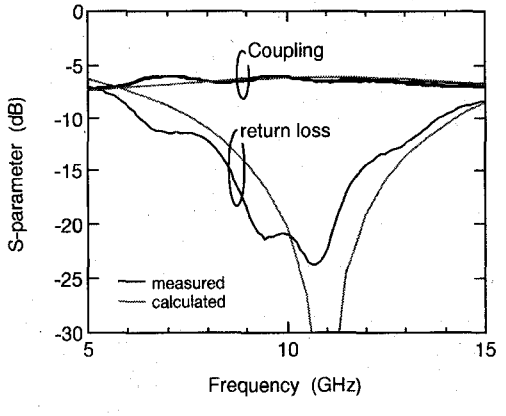

Fig. 11. Measured performance of the four-port divider.

spectively, the width and height of lower and upper conductor. The coupler is constructed with a strip conductor on the third and fourth polyimide layers, and ground metal on the alumina-ceramic substrate. Tight coupling (3 dB) is provided by appropriately choosing the heights and widths of the upper and lower strips. For a 3-dB coupler with characteristic impedance $Z_0 = 50\ \Omega$, $Z_{0e} = 121\ \Omega$ and $Z_{0o} = 21\ \Omega$ are required, where Z_{0e} and Z_{0o} denote the characteristic impedance of even- and odd-mode, respectively. Fig. 12(b) shows the characteristic impedance of each mode as calculated by the finite element method when $h_1 = 70\ \mu$m, $h_2 = 95\ \mu$m and $w_1 = 100\ \mu$m. The figure yields the solution "$w_2 = 80\ \mu$m". A photograph of a fabricated 10 GHz broadside coupler with intrinsic chip size of 0.8 mm × 1.7 mm is shown in Fig. 13. A meander-like configuration, shown in Fig. 12, is used to reduce the chip size drastically, as it does for the four-port divider. The measured and calculated performance of the coupler is shown in Fig. 14. Coupling loss of 3.3 ± 0.5 dB, and return and isolation losses of better than 15 dB are obtained at frequencies between 6.5 GHz and 11 GHz. The phase difference of the output signals between port ② and port ③ is 90 ± 5 degrees over the 6–14 GHz frequency band. The broadside coupler achieves a very low insertion loss of 0.3–0.4 dB, which is five times lower than that ever reported for broadside couplers [21] fabricated on 3-D MMIC structures because of the conductors' width. The measured coupling characteristic is narrower than the calculated one because the thickness of the fourth polyimide layer was, due to manufacturing error, more than 2 μm greater than designed. Measured results show that the multilayer substrate can realize very compact and low-loss IF hybrids for antenna array systems.

VI. Discussion

By using hybrid technology, the alumina-ceramic/polyimide multilayer substrate has great potential to achieve active anten-

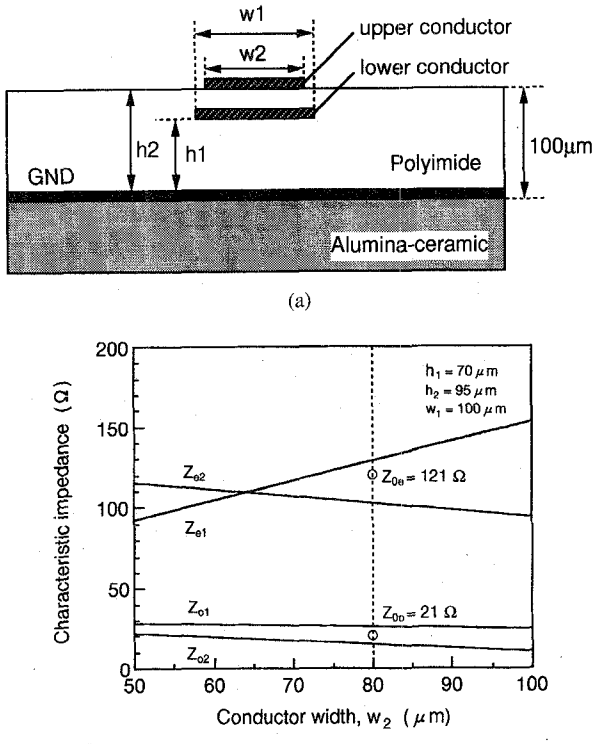

Fig. 12. Cross section and design chart of the broadside coupler.

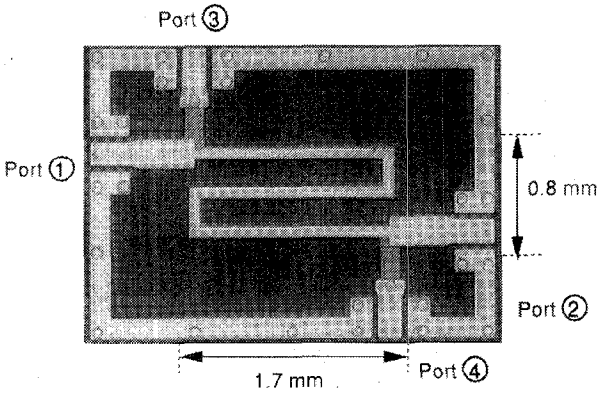

Fig. 13. Photograph of the 10 GHz 90° broadside coupler.

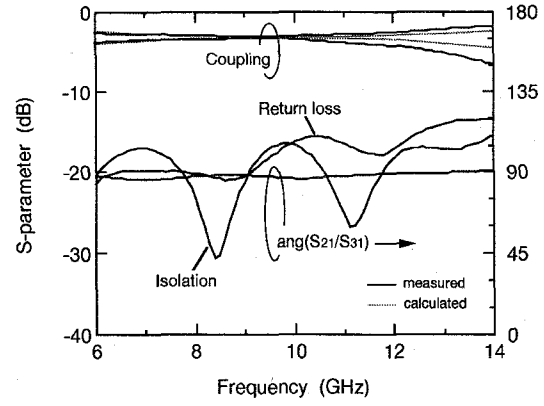

Fig. 14. Measured performance of the broadside coupler.

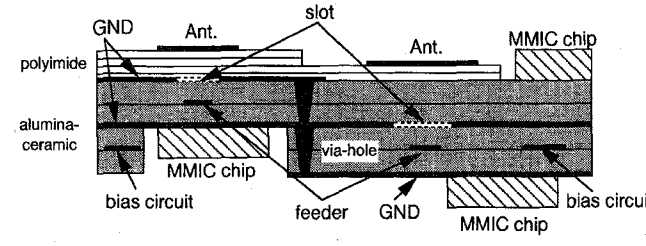

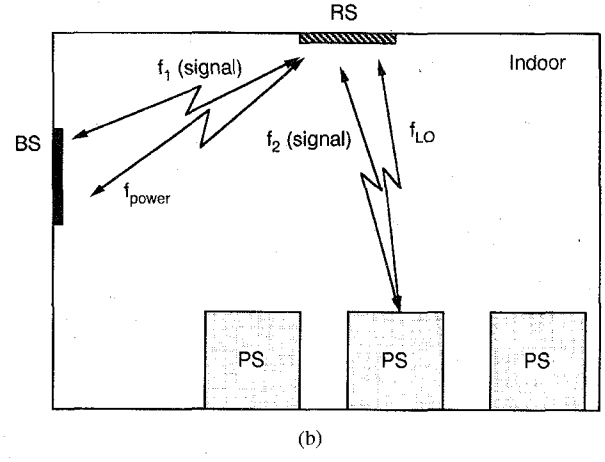

Fig. 15. Active antenna applications: (a) configuration and (b) indoor wireless LAN system.

nas integrated with solid-state devices and MMIC's because of features 1), 2), 4), and 5), as well as the above measured results of antennas and power combining circuits. The active antenna systems integrated with MMIC's on ceramic/polyimide substrate, shown in Fig. 15(a), provide several special benefits. First, it is more flexible to mount MMIC's on the substrate as shown in Fig. 15(a) because the polyimide and ceramic layers can be removed selectively. Second is the support of bias circuits as well as feeders. In addition, the substrate combined with thin film capacitors [13] elminate the chip capacitors previously needed in the bias circuits of MMIC's. The feeding methods considered are microstrip feed, via feed and electromagnetical coupling feed, and so on. Therefore, the multilayer configuration can also be easily used for designing slot-coupled microstrip antennas [1] suitable for antenna/MMIC's integration, as shown in Fig. 15(a).

Dual-frequency and multifrequency operation antennas provide a number of applications such as mixers, diplexers and transponders with MMIC's. The proposed antenna configuration has no basic limitation on the number of frequencies possible, so other applications are possible, e.g., millimeter-wave communication systems, in which high frequency operation signals are controlled by microwave signals. Fig. 15(b) shows another example, i.e., indoor wireless communication systems [22] in which relay stations (RS's) mounted on the ceiling communicate with the base station (BS) and personal stations (PS's) at different frequencies. Because the dual-frequency and multifrequency antennas fabricated on multilayer substrates occupy only one side of the substrate, we can realize simpler and more cost-effective RS's. Furthermore, by adding communication paths for LO signal and power supply lines to an RS,

it is possible to achieve a perfect no-wiring (no source-power) RS's mounted on the ceiling.

VII. Conclusion

We have presented a new multifrequency microstrip antenna method that uses an alumina-ceramic/polyimide multilayer dielectric substrate, and demonstrated two frequency-band antennas and two power combining circuits. Both antennas were fabricated and found to perform well, indicating that the multilayer configuration is very useful for multifrequency antenna design. A broadside coupler and divider designed on this multilayer substrate were comfirmed to offer low-insertion-loss and wideband chracteristics so arrays with high efficiency are now feasible. Finally, the possibility of applying this technology to active antennas was discussed. Given the measured results and our discussion, antenna systems built on the multilayer substrate with active devices and MMIC's, are promising for various active antenna applications.

Acknowledgment

The authors would like to thank Dr. K. Kohiyama of NTT Wireless Systems Laboratories for his continuous support and encouragement, and Dr. T. Hori, Dr. I. Toyoda, and Mr. K. Nishikawa of NTT Wireless Systems Laboratories for several active discussions.

References

[1] D. M. Pozar, "Microstrip antenna aperture coupled to a microstrip line," *Electron Lett.*, vol. 21, no. 2, pp. 49–50, 1985.
[2] R. J. Mailloux, "Phased array architecture for mm-wave active arrays," *Microwave J.*, pp. 117–124, July 1986.
[3] J. Huang, D. Rascoe, A. L. Riley, V. Ludecke, and L. Dufy, "A Ka-band MMIC phased array antenna," in *1989 IEEE AP-S Dig.*, pp. 1212–1215.
[4] H. Ohmine, T. Kashiwa, and M. Matsunaga, "An MMIC aperture-coupled microstrip antenna in the 40 GHz band," *1992 IEEE AP-S*, pp. 1105–1108.
[5] S. A. Long and M. D. Walton, "A dual-frequency stacked circular-disc antenna," *IEEE Trans. Antenna Propagat.*, AP-27, pp. 270–273, Mar. 1979.
[6] J. S. Dahele, K. F. Lee, and D.P. Wong, "Dual frequency stacked annular-ring microstrip antenna," *IEEE Trans. Antenna Propagat.*, AP-35, pp. 1281–1285, Nov. 1987.
[7] J. Wang, R. Fralich, C. Wu, and J. Litva, "Multifunctional aperture coupled stack antenna," *Electron. Lett.*, vol. 26, no. 25, Dec. 1990.
[8] F. Croq and D. M. Pozar, "Multifrequency operation of microstrip antennas using aperture coupled parallel resonators," *IEEE Trans. Antenna Propagat.*, vol. 40, no. 11, pp. 1367–1374, Nov. 1992.
[9] K. Kamogawa, T. Tokumitsu, and M. Aikawa, "A novel microstrip antenna using alumina-ceramic/polyimide multilayer dielectric substrate," *1996 IEEE MTT-S Dig.*, pp. 71–74.
[10] K. Kamogawa and T. Tokumitsu, "A Novel Antenna Using Ceramic/Polyimide Multilayer Dielectric Substrate," IEICE Tech. Rep., vol. 95, no. 178, MW95-47, pp. 1–6, 1995 (in Japanese).
[11] A. Dohya, T. Watari, and H. Nishimori, "Packaging technology for the NEC SX-3/SX-X supercomputer," in *Proc. IEEE 1990 40th Electronic Components Technol. Conf.*, pp. 525–533.
[12] W. Volksen, D. Y. Yoon, J. L. Hedrick, and D. Hofer, *Mat. Res. Soc. Symp. Proc.*, vol. 227, p. 23, 1991.
[13] R. Kambe, R. Imai, T. Takada, M. Arakawa, and M. Kuroda, "MCM substrate with high capacitance," *IEEE Trans. Comp., Packag. Manufact., Technol B,* vol. 18, no. 1, pp. 23–27, Feb. 1995.
[14] N. Iwasaki and S. Yamaguchi, in *Proc. IEEE CHMT Jap. IEMT Symp.*, 1989, p. 128.
[15] I. J. Bahl and P. Bhartia, *Microstrip Antennas.* Dedham, MA: Artech House, 1980.
[16] D. M. Pozar, "Considerations for millimeter wave printed antennas," *IEEE Trans. Antenna Propagat.*, vol. 31, pp. 740–747, Sept. 1983.
[17] M. Kominami and K. Rokushima, *IEICE Trans. Communications*, vol. J-69-B, 9, pp. 941–948, 1986 (in Japanese).
[18] T. Tokumitsu, T. Hiraoka, H. Nakamoto, and M. Aikawa, "Multilayer MMIC using a 3 μm $\times N$-layer dielectric film structure," *IEICE Trans. Electron.*, vol. E75-C, pp. 713–720, June 1992.
[19] S. Banba and H. Ogawa, "Small-sized MMIC amplifiers using thin dielectric layers," *IEEE Trans. Microwave Theory Tech.*, vol. 43, no. 3, pp. 485–492, Mar. 1995.
[20] T. Tokumitsu, K. Nishikawa, K. Kamogawa, I. Toyoda, and M. Aikawa, "Three-dimensional MMIC technology for multifunction integration and its possible application to masterslice MMIC," *1996 IEEE Microwave Millimeter-Wave Monolithic Circ. Symp. Dig.*
[21] I. Toyoda, T. Hirota, T. Hiraoka, and T. Tokumitsu, "Multilayer MMIC branch-line coupler and broad-side coupler," in *IEEE 1992 Microwave Millimeter-Wave Monolithic Circuits Symp. Dig*, pp. 79–82.
[22] K. Uehara, T. Seki, and K. Kagoshima, "New indoor high-speed radio communication system," in *1995 IEEE 45th Veh. Technol. Conf. Dig.*, pp. 996–1000.

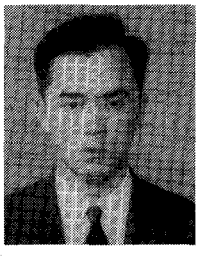

Kenji Kamogawa (M'93) was born in Ehime, Japan, in 1967. He received the B.E. and M.E. degrees in electorical engineering from University of Osaka Prefecture, Osaka, Japan, in 1990 and 1992, respectively.

He joined NTT Radio Communication Systems Laboratories, Yokosuka, Japan, in 1992. Since 1994, he has been with NTT Wireless Systems Laboratories. He has been engaged in research on GaAs MMIC's and their expansions to antenna-MMIC integration and 3-D integration.

Mr. Kamogawa is a member of the Institute of Electronics, Information and Communication Engineering (IEICE) of Japan.

Tsuneo Tokumitsu (M'88), for a photograph and biography, see this issue, p. 2346.

Masayoshi Aikawa (M'78), for a photograph and biography, see this issue, p. 2346.